

Published in final edited form as:

Clin Neurophysiol. 2014 September ; 125(9): 1764–1773. doi:10.1016/j.clinph.2014.01.021.

Eye closure causes widespread low-frequency power increase and focal gamma attenuation in the human electrocorticogram

Aaron S. Geller¹, John F. Burke², Michael R. Sperling³, Ashwini D. Sharan⁴, Brian Litt⁵, Gordon H. Baltuch⁶, Timothy H. Lucas II⁶, and Michael J. Kahana¹

¹Department of Psychology, University of Pennsylvania 19104

²Department of Neuroscience Graduate Group, University of Pennsylvania 19104

³Department of Neurology Thomas Jefferson University 19107

⁴Department of Neurological Surgery, Thomas Jefferson University 19107

⁵Department of Neurology University of Pennsylvania School of Medicine 19104

⁶Department of Neurosurgery, University of Pennsylvania School of Medicine 19104

Abstract

Objective: We sought to characterize the effects of eye closure on EEG power using electrocorticography (ECoG). Specifically, we sought to elucidate the anatomical areas demonstrating an eye closure effect, and at which frequencies these effects occur.

Methods: ECoG was recorded from 32 patients undergoing invasive monitoring for seizure focus localization. Patients were instructed to close and open their eyes repeatedly. ECoG power was compared in the epochs following eye closure and opening, for various frequency bands and brain regions.

Results: We found that at low frequencies, eye closure causes widespread power increases involving all lobes of the brain. This effect was significant not only in the α (8–12 Hz) band but in the δ (2–4 Hz), θ (4–8 Hz), and β (15–30) bands as well. At high frequencies, eye closure causes comparatively focal power decreases over occipital cortex and frontal Brodmann areas 8 and 9.

Conclusions: Eye closure (1) affects a broad range of frequencies outside the α band and (2) involves a distributed network of neural activity in anatomical areas outside visual cortex.

Significance: This study constitutes the first large-scale, systematic application of ECoG to study eye closure, which is shown to influence a broad range of frequencies and brain regions.

© 2014 International Federation of Clinical Neurophysiology. Published by Elsevier Ireland Ltd. All rights reserved

Correspondence should be addressed to: Aaron S. Geller (aaron.geller@nyumc.org) NYU Langone Medical Center Department of Neurology NBV 7W11 462 1st Ave. New York, NY 10016 Phone: (212) 263-7744, Fax: (212) 263-7721.

Publisher's Disclaimer: This is a PDF file of an unedited manuscript that has been accepted for publication. As a service to our customers we are providing this early version of the manuscript. The manuscript will undergo copyediting, typesetting, and review of the resulting proof before it is published in its final citable form. Please note that during the production process errors may be discovered which could affect the content, and all legal disclaimers that apply to the journal pertain.

Conflict of Interests: The authors declare no competing financial interests.

Keywords

Intracranial EEG; ECoG; eye closure; event-related synchronization; alpha; gamma; high frequency activity; frontal eye fields

Introduction

Eye closure is the single most effective behavioral modulator of the human electroencephalogram (EEG), an effect as old as EEG itself (Berger, 1929). This effect is qualitatively described by a transition from low-amplitude, non-rhythmic electrical activity to high-amplitude, oscillatory activity during the period of eye-closure. The early, now classic, investigations describing this effect identified the frequency band of the oscillatory component during eye-closure as the “alpha” wave (Berger, 1929); these studies isolated the effect specifically to visual stimulation (Adrian and Matthews, 1934) and also provided evidence that α oscillations originated in the occipital lobes (Adrian and Yamagiwa, 1935). Additional studies confirmed this effect and provided evidence on its ubiquity and reliability (Jasper, 1936; Smith, 1938; Jasper and Andrews, 1938).

The studies that followed up on these basic findings can be divided into two lines of research: those recording non-invasively from human participants and those recording invasively from animal models. In the first, the principal questions were whether the eyes-closed condition modulated (1) spectral activity outside of the α band and (2) regional activations outside of visual cortex. Using scalp EEG, it was indeed found that activity outside of the α band, namely in the δ , θ , and β bands, was also modulated by the eyes-closed condition (Chapman et al., 1962; Glass and Kwiatkowski, 1970; Hardle et al., 1984). In addition, the temporal and parietal lobes displayed eyes-closed related activity, albeit at different resonant frequencies than the visual cortical α modulation (Mundy-Castle, 1957; Volavka et al., 1967; Legewie et al., 1969). Despite these advances, however, this line of research was severely limited by the poor spectral and spatial resolution of scalp EEG. For example, it was not possible in the early scalp recordings to relate γ activity to the eyes-open condition, despite the fact that γ activity has been explicitly related to visual processing (Jensen et al., 2007). As a result of these technical limitations, modern research has focused on the higher-level cognitive correlates of α activity (Mantini et al., 2007; Klimesch et al., 1996; VanRullen et al., 2005; Busch et al., 2009; Jensen et al., 2012). As a result, many basic electrophysiological properties of eye-closure in humans remain unknown.

The second line of research responded to the inherent limitations of using scalp studies to investigate visual cortical α -activity. To overcome these limitations, these studies investigated the α rhythm using invasive electrophysiology in animal models, opening the skull to obtain direct recordings from neural tissue (reviewed in Lopes Da Silva, 1991). Using this approach, early studies suggested that the α rhythm emerged from sub-cortical structures, namely the lateral geniculate nucleus, the pulvinar and the reticular activating system (Andersen and Andersen, 1968). However, it was soon appreciated that cortical generators uniquely contributed to the α effect (Lopes Da Silva et al., 1973; Lopes Da Silva and van Leeuwen, 1977; Bollimunta et al., 2008, 2011). Despite the advances from this line

of research, it remains a challenge to apply these findings directly to the human brain. In particular, recordings in animal models are usually performed using micro-electrodes confined to highly specific regions of the thalamus and visual cortex. Therefore, the question of precisely which anatomical regions (outside of the visual cortex) respond to eye-closure has largely been unexplored.

To overcome the challenges of each of these lines of research, it is necessary to record invasively electrophysiological activity directly from the human brain as participants open and close their eyes. Such recordings can be ethically obtained from neurosurgical patients undergoing invasive monitoring for seizure localization in the setting of pharmacologically resistant epilepsy. Indeed, intracranial EEG, or electrocorticography (ECoG), has been used to elucidate the neural activity of a variety of motor, sensory, and cognitive phenomenon (Jacobs and Kahana, 2010; Lachaux et al., 2012), but has yet to be systematically applied to the most basic of all electrophysiological behavioral effects: human eye-closure. By recording directly from the surface of the brain, much like the animal models described above, ECoG can localize cortical eye closure effects with maximal anatomical precision. In addition, ECoG has the potential to record high-frequency activity (γ) in the absence of muscular artifact that occurs at the scalp (Yuval-Greenberg et al., 2008).

In this study, we examined the effect of eye closure on ECoG power during a simple eye closure/eye opening task. In it, we sought to examine both the spatial distribution of cortical responses to eye closure and opening, as well as which frequencies participated in the response.

Materials and Methods

Participants

32 patients (13 female, 4 left-handed; Table 1) with pharmacologically-refractory epilepsy underwent a surgical procedure in which electrodes were implanted subdurally on the cortical surface; many of these patients received implants deep within the brain parenchyma as well. In each case, the clinical team determined the placement of the electrodes so as to best localize epileptic foci. Data were collected at the Hospital of the University of Pennsylvania (Philadelphia, PA) and Thomas Jefferson University Hospital (Philadelphia, PA). Our research protocol was approved by the institutional review board at both hospitals and informed consent was obtained from the participants and their guardians.

Behavioral Task

Each patient participated in a suite of oculomotor tasks lasting, in total, 5-10 minutes (Figure 1A, top-panel). These tasks engaged the facial and extraocular muscles as well as the systems subserving saccades and smooth pursuit. The first and last elements in this suite were an alternating series of instructions for the patient to close and open his or her eyes. In the current paper, we have analyzed data only from these two elements, heretofore referred to as the eye-closure task. In the eye-closure task, asterisks are drawn on the screen at the 12, 3, 6 and 9 o'clock positions, and the pre-recorded words "close" and "open" are played in sequence 5 times (Figure 1A, bottom-panel). The duration of the "close" and "open" clips

are approximately 1480 and 1400 ms, respectively. Each word is followed by a delay interval of 5000 ms + uniformly-distributed jitter drawn from the interval [0, 300] ms.

ECoG recordings

Data from our 32 patient database were collected over a 6-year period in collaboration with 2 different hospitals. Whereas each hospital used the same general implantation procedures and data-acquisition techniques, our analysis had to account for technical details that varied by institution. Electroencephalography (ECoG) data were recorded using a Nicolet, Grass Telefactor, or Nihon-Khoden EEG system. Depending on the amplifier and the discretion of the clinical team, the signals were sampled at 400, 500, 512, 1000, or 2000 Hz. Signals were referenced to a common electrode placed either intracranially or on the scalp or mastoid process. All recorded traces were re-sampled at 256 Hz, and a fourth order 2-Hz stop-band Butterworth notch filter was applied at 60 Hz to eliminate electrical line noise. The experimental laptop sent ± 5 V analog pulses, via an optical isolator, into a pair of open lines on the clinical recording system to synchronize the electrophysiological recordings with behavioral events.

We collected electrophysiological data from a total of 3,333 subdural and depth electrodes (1,614 left-hemispheric; 1,719 right hemispheric). Subdural electrodes were arranged in both grid and strip configurations with an inter-electrode spacing of 10 mm (Figure 1B). Depth electrodes (6-8 platinum contacts) were placed in 20/32 patients; all depth electrodes were placed in the medial temporal lobe except for one patient whose depth electrodes were placed in superior temporal gyrus near auditory cortex (TJUH 20; see Table 1). Electrode localization was accomplished by first localizing the implanted electrodes on the post-operative computed tomography (CT). Then, the CT was co-registered with magnetic resonance images (MRI) and assigned standardized three dimensional Montreal Neurological Institute (MNI) and Talairach coordinates using the FLIRT registration (FSL software package; Boston, MA). Using the Talairach coordinates, each electrode was labelled with a Brodmann area using the Talairach Daemon (Lancaster et al., 2000). Details regarding each patient's electrode montage, behavioral performance, and amplifier filter settings can be found in Table 1.

We use bipolar referencing to eliminate (1) sources of noise common to adjacent electrodes (Nunez and Srinivasan, 2006) and (2) the contribution of eye-muscular artifacts to the electrophysiological recording (Kovach et al., 2011). We defined the bipolar montage in our data-set based on the geometry of ECoG electrode arrangements. For every grid, strip and depth probe, we isolated all pairs of electrodes that were positioned immediately adjacent to one another; bipolar signals were then found by differencing the signals between each pair of immediately adjacent electrodes (Anderson et al., 2010; Burke et al., 2013). The resulting bipolar signals were treated as new virtual electrodes, originating from the mid-point between each electrode pair. All subsequent analyses were performed using these derived bipolar signals.

Data Analysis and Spectral Power

Time-domain values were z -transformed with respect to the session-wise mean and standard deviation, to account for changes in power across sessions. To quantify behaviorally-related changes in spectral power, we convolved the down-sampled (256 Hz) bipolar ECoG signals with complex-valued Morlet wavelets (wave number 6) to obtain magnitude and phase information (Addison, 2002). Each wavelet was convolved with 8500 ms of ECoG data, starting at each presentation of the word “close” or “open” (a 1000 ms buffer was included on both sides of the clipped data). We used between 49 and 60 wavelets with center frequencies logarithmically spaced between 2 to 400 Hz, as the sampling rate of the particular recording would allow, with extra wavelets added at higher frequencies. The wavelet was used to transform the voltage trace at each electrode to an instantaneous power trace for each frequency. These frequency-domain values were then log-transformed.

For the frequency-band analysis, we averaged the resulting z -transformed instantaneous powers into six frequency bands of interest: delta (δ : 2–4 Hz), theta (θ : 4–8 Hz), alpha (α : 8–12 Hz), beta (β : 15–30 Hz), gamma (γ : 30–58 Hz), and high-frequency activity (HFA: 62–120 Hz). HFA was used because of many recent studies that have shown that activity in this frequency band is uniquely related to underlying multi-unit activity (Manning et al., 2009; Miller et al., 2009; Ray and Maunsell, 2011). Two frequency bands were of particular interest for this task, namely, α and γ . To visualize instantaneous power effects for α and γ across multiple sequential close/open pairs (Figure 2), the instantaneous power was calculated as described above using 80,000 ms of ECoG data (throughout an entire trial of the eye closure task; see Figure 1A). Power in each band was then averaged across all electrodes in a particular region (anatomical lobe; see Figure 2).

Anatomical localization

To visualize the anatomic variability of behaviorally-correlated power effects, for each electrode, the mean power at all frequencies was computed for each pair of “close” and “open” events for the interval between 4400 and 6400 ms post-stimulus. For each pair of events, this produced $2f \times s$ matrices per electrode, E_{open} and E_{closed} , where f is the number of frequencies and s the number of samples. For each E_{open} and E_{closed} , the mean power over time was then taken, producing two $f \times 1$ matrices. The f values in each matrix were then averaged into the frequency bands described above, such that each electrode contributed $2b \times 1$ matrices, $E_{open,coll}$ and $E_{closed,coll}$, where the subscript “*coll*” indicates collapsing over time and frequencies. These matrices were averaged over the n electrodes recording from the specific region for the given subject, producing a single pair of matrices $open,coll$ and $closed,coll$ for each subject with coverage in the given Brodmann area. The effect of eye closure at a given Brodmann area was then computed by comparing the across-subject grand mean at each frequency band for the 2 conditions:

$$\bar{X}_{closed,coll} = \frac{\sum \bar{E}_{close,coll}}{n}$$

and

$$\bar{X}_{open,coll} = \frac{\sum \bar{E}_{open,coll}}{n},$$

where n is the number of subjects with electrodes in the given Brodmann area. $\bar{X}_{closed,coll}$ and $\bar{X}_{open,coll}$ were compared with a paired-samples t -test. A threshold of $n = 5$ subjects contributing to a Brodmann area was required for that area to be included. In this analysis, multiple comparisons were controlled for using the FDR method (Benjamini and Hochberg, 1995) with q set to 0.05.

Results

Our goal was to investigate the effect of eye closure on the human ECoG. We were particularly interested in which regions outside of primary visual cortex exhibited an electrophysiological response to eye closure and whether high frequencies were modulated by the task. To accomplish this, we administered a behavioral task in which participants were asked repeatedly to close and open their eyes (Figure 1A); participants were neurosurgical patients undergoing intracranial monitoring for the localization of their seizure focus using implanted subdural electrodes (Figure 1B). During the task, we recorded ECoG data from the electrodes and examined which spectral frequencies were modulated as the patient closed and opened their eyes.

Eye closure has been shown across a variety of tasks to modulate the amount of α power in electrophysiological recordings. α modulation during the eyes open-close manipulation was occasionally visible in raw ECoG data; for example, Figure 1C demonstrates an α pattern that was induced one second after the patient was instructed to close her eyes. Aside from such α effects, we were also interested in whether eye-closure also modulated the power in intracranial high-frequency activity, which may not be detectable from visual inspection alone. We therefore first investigated the degree to which these two frequencies, α (8–12 Hz) and γ (30–120 Hz) increased or decreased, across all electrodes in our database, during the task. First, to obtain a qualitative sense of the effect eye closure has on α and γ power, we plotted the instantaneous α and γ power across all electrodes in each of these bands against time, separately for each anatomical region-of-interest (Figure 2). This analysis revealed that eye closure generally tends to augment α power and diminish γ power, and that both of these effects occur on the timescale of approximately 2s after eye closure. The α power effect, though clearly largest over occipital cortex, is visible over parietal and temporal cortex as well as the hippocampus, and to a lesser degree over frontal cortex. The γ power effect, by contrast, is prominent over occipital cortex and to a lesser degree over parietal cortex.

Figure 2 shows that α and high-frequency activity are both modulated by eye-closure, and we next wanted to investigate more precisely which frequencies are involved in such modulation. To evaluate the electrophysiological response in other frequency bands, we calculated the region-wise power-spectral density for each close/open event (PSD; left-hand column of Figure 3). As is visible in Figure 2, the effects of both eye closure and opening

are maximal approximately 4s post-instruction; for this reason, the epoch between 4400 and 6400 ms was used to compare power between the eyes-closed and eyes-open conditions in the PSD analysis. For each region, for each participant, a PSD was computed for each electrode in the region corresponding to eyes closed and eyes open during the aforementioned interval. This analysis demonstrates that there are two processes pertinent to power changes associated with eye closure. The first is a narrowband effect present primarily over occipital cortex (to a much smaller degree over parietal cortex), visible as a local α band peak in the eyes-closed PSD for the occipital lobe. The second is a broadband shift which causes an overall divergence in the PSDs at several low frequencies, leading to the eyes-closed PSDs to remain parallel to the eyes-open PSDs. This effect is visible over occipital, parietal, temporal and hippocampal cortices. Finally, the PSDs demonstrate that eye opening is associated with augmentation of power at high frequencies, visible as an intersection of the power spectra at approximately 32 Hz.

To investigate how the PSDs in the left column of Figure 3 varied as a function of the time relative to the eyes open/close command, we calculated the difference in the eyes open/close PSDs at each frequency and instantaneous time sample. The resulting time frequency plots are shown Figure 3, right panel. The time-frequency plots show that the changes in the PSDs are relatively constant across time and appear to be a general property of the eyes open/close behavioral state as opposed to, say, a transition between one state to the next.

The principal advantage which ECoG provides over scalp EEG is spatial resolution, and we sought to leverage this advantage to localize precisely the regions that are affected by eye closure. To do this, we compared power after eye closure and opening (for the above-mentioned interval) at the Brodmann area level. This analysis (Figure 4) shows that the low-frequency power increase associated with eye closure is diffuse both regarding its spatial and spectral extent. This power increase is significant over large bilateral swaths of occipital, temporal and parietal cortex as well as both hippocampi in all of the low frequency bands. Several frequency-specific effects are also observed: the increase over BA 18 is significant only in the α and β bands, and is stronger on the right. Prominent frontal increases are significant in the θ band bilaterally (BAs 4, 6, 10 and 46 on the left; and 4, 6, 9 and 46 on the right), and in the β band on the right (areas 4, 6, 8 and 9). Also, high-frequency power decreases are most prominent at high γ (here defined as 62-120 Hz) in Brodmann areas 8, 18 and 19 bilaterally.

Discussion

In this study we examined the spectral signature of eye closure in a cohort of epilepsy patients undergoing invasive monitoring. Patients were instructed to close and open their eyes multiple times in sequence. We report 4 findings. First, eye closure is associated with significant power increases not only in the α band, but in all low-frequency bands, from the δ -band (2-4 Hz) to the β -band (15-30 Hz). Second, the power effect of eye closure is spatially diffuse, involving temporal and parietal cortex as well as both hippocampi. Third, peaks corresponding to α oscillations are visible in the mean PSDs for occipital, and to a lesser degree, parietal, cortex. Fourth, the broadband low-frequency power increase with eye closure occurs with a simultaneous high-frequency power decrease. In contrast to the low-

frequency power increase, the high-frequency power decrease was highly specific anatomically, located over occipital cortex and Brodmann area 8 bilaterally.

Since the first observation that eye closure increases the amount of α oscillatory power over posterior electrodes in the scalp electroencephalogram (Berger, 1929; Jasper and Andrews, 1938; Jasper and Penfield, 1949), there have been a number of studies examining the relation between α power and eye-closure (Mundy-Castle, 1957; Volavka et al., 1967; Legewie et al., 1969; Chapman et al., 1962; Glass and Kwiatkowski, 1970; Hardle et al., 1984). Most of these studies attempted to identify the generator of the α oscillation, which was initially proposed to involve the thalamus (Andersen and Andersen, 1968) and later suggested to derive from neocortical sources (Lopes Da Silva et al., 1973; Lopes Da Silva and van Leeuwen, 1977; Bollimunta et al., 2008, 2011). However, relatively few studies have systematically studied the effect of eye-closure on frequencies outside of the α band. Using scalp EEG, Barry and colleagues have identified low frequencies outside of the α band and visual cortical areas that are similarly modulated by eye-closure (Barry et al., 2007, 2009). Here, by performing the first systematic evaluation of the effect of eye-closure on human intracranial electrophysiology, we were able to extend these findings. Specifically, direct brain recordings allowed us to investigate (1) whether frequencies in the γ range were also modulated by eye-closure and (2) the spatial location of all such spectral modulations.

With regard to the γ frequency findings, we found that eye closure is associated with a reliable decrease in high-frequency power. Coupled with the increase in low-frequency power, these data suggest that eye closure participates in an electrophysiological motif defined by a skew in power toward low frequencies at the expense of high frequencies. Assuming the eyes-open condition represents the active component of this behavior, then these results can be conceptualized as an increase in γ alongside a decrease in δ , θ , α , and β frequencies. This electrophysiological pattern, often labelled event related synchronization/desynchronization (ERS/ERD) (Pfurtscheller and Lopes Da Silva, 1999), is often observed during the active component of many behaviors including movement and other motor functions (Pfurtscheller and Aranibar, 1979; Pfurtscheller and Neuper, 1992; N. E. Crone, Miglioretti, Gordon, and Lesser, 1998; N. E. Crone, Miglioretti, Gordon, Sieracki, et al., 1998; Graitmann et al., 2002; Miller et al., 2007), auditory perception (N. Crone et al., 2001), sensory tasks (Cheyne et al., 2003; Gaetz and Cheyne, 2006; Freyer et al., 2013), visual perceptual activities (Hipp et al., 2011), memory formation (Burke et al., 2014), and many others. The ubiquity of this pattern has led researchers investigating animal models of activation to suggest that this pattern represents a movement from a less to a more activated cortical state (Poulet and Petersen, 2008; Poulet et al., 2012). Here, we suggest that an analogous interpretation explains the current findings, i.e. the increase in high-frequency power and decrease in low-frequency power during the transition from eyes-closed to eyes-open represents a cortical state transition (Harris and Thiele, 2011).

The second major novel aspect of this work involves the use of direct brain recordings to investigate the spatial location of the spectral modulations during eye closure. We found that eye closure modulated activity of low-frequency activity well outside of visual areas (see also Barry et al., 2007). Here, we find structures such as the temporal cortex, the frontal

cortex, and even the hippocampus are modulated by eye closure. These data suggest that visual activation triggers an anatomically widely-distributed network, one which includes areas that have not been classically implicated in visual processing. A second striking result is the high-frequency deactivation on eye closure (activation on eye opening) of Brodmann area 8 bilaterally. The regions modulated at high frequencies are highly circumscribed in comparison with the broad swaths of cortex modulated at low frequencies. BA 8 is known to contain at least part of the Frontal Eye Fields (FEFs; Stanton et al., 1989), which are implicated in both visually-related motor activity and top-down visual attention (Schafer and Moore, 2007; Gregoriou et al., 2009). These findings provide a link between the electrophysiological effects of eye-opening and studies of top-down visual attention (Buschman and Miller, 2007).

In presenting the ECoG effects of eye closure, we acknowledge, first, that our cortical picture is not comprehensive, and secondly, that the cortical effects reported reflect input from two sources whose activity we have not recorded, specifically the thalamus and brain stem. Our cortical picture is particularly limited most notably in its coverage of Brodmann area 17, which would be of great interest in examining eye closure effects. The role of the thalamus in α oscillation was mentioned above and is still being elucidated. Modulation of the EEG by brainstem inputs is an effect demonstrated by the classic *cerveau isolé* preparation of Bremer (1935), which anticipated the discovery of the reticular activating system and its influence on the EEG (Moruzzi and Magoun, 1949). Of particular interest is the influence of the midbrain, which receives visual input via the extrageniculate visual pathway.

This study is the first to analyze human direct brain recordings during the eyes-open/closed manipulation. This approach yielded a number of novel findings, as described above, and also promises many additional insights. In particular, it is currently unclear if γ activity in the FEF follows or is followed by activity in the visual areas during the eyes open condition. The direction of this interaction is particularly important because it will help determine whether the observed changes represent top-down or bottom-up activations. A second important area of future research will be to determine the extent to which the narrow band modulations of α oscillations over visual cortex and the more diffuse broadband shifts in low-frequency power (Figure 3) represent two distinct processes. One significant development in the study of α in recent years is the mounting evidence for an active, inhibitory role for α oscillations. These findings have tended to emphasize narrow-band α inhibition (Jensen and Mazaheri, 2010; Jokisch and Jensen, 2007), but some have observed low-frequency broadband activity to be inhibitory (Bauer et al., 2012). The studies mentioned, it should be noted, all involve a cognitive load not present in the task studied here. Further work is necessary to clarify to what extent eye closure participates in the inhibitory mode of α .

Acknowledgments

This work was supported by National Institutes of Health Grants MH55687 and NS067316. We thank Ryan Williams for assistance with data collection; Dale H. Wyeth and Edmund Wyeth for technical assistance at Thomas Jefferson University Hospital. We are indebted to all patients who have selflessly volunteered their time to participate in our study.

References

- Addison, PS. The illustrated wavelet transform handbook: introductory theory and applications in science, engineering, medicine and finance. Institute of Physics Publishing; Bristol: 2002.
- Adrian ED, Matthews BHC. The berger rhythm: Potential changes from the occipital lobes in man. *Brain*. 1934; 57(4):355–85.
- Adrian ED, Yamagiwa D. The origin of the berger rhythm. *Brain*. 1935; 58:323–351.
- Andersen, P.; Andersen, SA. Physiological basis of the alpha rhythm. Appleton Century Crofts; New York: 1968.
- Anderson KL, Rajagovindan R, Ghacibeh G, Meador KJ, Ding M. Theta oscillations mediate interaction between prefrontal cortex and medial temporal lobe in human memory. *Cereb Cortex*. 2010; 20(7):1604–1612. [PubMed: 19861635]
- Barry RJ, Clarke AR, Johnstone SJ, Brown CR. EEG differences in children between eyes-closed and eyes-open resting conditions. *Clin Neurophysiol*. 2009; 120:1806–1811. [PubMed: 19748828]
- Barry RJ, Clarke AR, Johnstone SJ, Magee CA, Rushby JA. EEG differences between eyes-closed and eyes-open resting conditions. *Clin Neurophysiol*. 2007; 118:2765–2773. [PubMed: 17911042]
- Bauer M, Kluge C, Bach D, Bradbury D, Heinze HJ, Dolan RJ, Driver J. Cholinergic enhancement of visual attention and neural oscillations in the human brain. *Curr Biol*. 2012; 22:397–402. [PubMed: 22305751]
- Benjamini Y, Hochberg Y. Controlling the False Discovery Rate: a practical and powerful approach to multiple testing. *J Royal Stat Soc B*. 1995; 57:289–300.
- Berger H. Über das Elektrenkephalogramm des menschen (On the human electroencephalogram). *Archiv für Psychiatrie und Nervenkrankheiten*. 1929; 87:527–570.
- Bollimunta A, Chen Y, Schroeder CE, Ding M. Neuronal mechanisms of cortical alpha oscillations in awake-behaving macaques. *J Neurosci*. 2008; 28(40):9976–9988. [PubMed: 18829955]
- Bollimunta A, Mo J, Schroeder CE, Ding M. Neuronal mechanisms and attentional modulation of corticothalamic alpha oscillations. *J Neurosci*. 2011; 31:4935–4943. [PubMed: 21451032]
- Bremer F. Cerveau “isolé” et physiologie du sommeil. *C R Seances Soc Biol Fil*. 1935; 119:1235–1241.
- Burke JF, Long NM, Zaghoul KA, Sharan AD, Sperling MR, Kahana MJ. Human intracranial high-frequency activity maps episodic memory formation in space and time. *NeuroImage*. 2014; 85:834–843. Pt. 2. [PubMed: 23827329]
- Burke JF, Zaghoul KA, Jacobs J, Williams RB, Sperling MR, Sharan AD, Kahana MJ. Synchronous and asynchronous theta and gamma activity during episodic memory formation. *J Neurosci*. 2013; 33(1):292–304. [PubMed: 23283342]
- Busch NA, Dubois J, VanRullen R. The phase of ongoing EEG oscillations predicts visual perception. *J Neurosci*. 2009; 29:7869–7876. [PubMed: 19535598]
- Buschman TJ, Miller EK. Top-down versus bottom-up control of attention in the prefrontal and posterior parietal cortices. *Science*. 2007; 315(5820):1860–1862. [PubMed: 17395832]
- Chapman RM, Armington JC, Bragdon HR. A quantitative survey of kappa and alpha EEG activity. *Electroenceph Clin Neurophysiol*. 1962; 14:858–68. [PubMed: 14020161]
- Cheyne D, Gaetz W, Garnero L, Lachaux JP, Ducorps A, Schwartz D, Varela FJ. Neuromagnetic imaging of cortical oscillations accompanying tactile stimulation. *Cognitive Brain Research*. 2003; 17(3):599–611. [PubMed: 14561448]
- Crone N, Boatman D, Gordon B, Hao L. Induced electrocorticographic gamma activity during auditory perception. *Clin Neurophysiol*. 2001; 112(4):565–582. [PubMed: 11275528]
- Crone NE, Miglioretti DL, Gordon B, Lesser RP. Functional mapping of human sensorimotor cortex with electrocorticographic spectral analysis. II. Event-related synchronization in the gamma band. *Brain*. 1998; 121(12):2301–2315. [PubMed: 9874481]
- Crone NE, Miglioretti DL, Gordon B, Sieracki JM, Wilson MT, Uematsu S, Lesser RP. Functional mapping of human sensorimotor cortex with electrocorticographic spectral analysis. I. Alpha and beta event-related desynchronization. *Brain*. 1998; 121:2271–2299. [PubMed: 9874480]

- Freyer F, Becker R, Dinse HR, Ritter P. State-dependent perceptual learning. *J Neurosci*. 2013; 33(7): 2900–2907. [PubMed: 23407948]
- Gaetz W, Cheyne D. Localization of sensorimotor cortical rhythms induced by tactile stimulation using spatially filtered MEG. *NeuroImage*. 2006; 30(3):899–908. [PubMed: 16326116]
- Glass A, Kwiatkowski AE. Power spectral density changes in the EEG during mental arithmetic and eye-opening. *Psychol Forsch*. 1970; 33:85–90. [PubMed: 5515904]
- Graimann B, Huggins JE, Levine SP, Pfurtscheller G. Visualization of significant ERD/ERS patterns in multichannel EEG and ECoG data. *Clin Neurophysiol*. Jan; 2002 113(1):43–47. [PubMed: 11801423]
- Gregoriou G, Gotts S, Zhou H, Desimone R. High-frequency, long-range coupling between prefrontal and visual cortex during attention. *Science*. 2009; 324(5931):1207–1210. [PubMed: 19478185]
- Hardle W, Gasser T, Bacher P. EEG responsiveness to eye opening and closing in mildly retarded children compared to a control group. *Biol Psych*. 1984; 18:185–99.
- Harris KD, Thiele A. Cortical state and attention. *Nat Rev Neurosci*. 2011; 12(9):509–523. [PubMed: 21829219]
- Hipp J, Engel A, Siegel M. Oscillatory synchronization in large-scale cortical networks predicts perception. *Neuron*. Jan; 2011 69(2):387–396. [PubMed: 21262474]
- Jacobs J, Kahana MJ. Direct brain recordings fuel advances in cognitive electrophysiology. *Trends Cog Sci*. 2010; 14(4):162–171.
- Jasper H. Cortical excitatory state and variability in human brain rhythms. *Science*. 1936; 83:259–260. [PubMed: 17757098]
- Jasper H, Andrews H. Electro-encephalography III. Normal differentiation of occipital and precentral regions in man. *Arch Neurol & Psych*. 1938; 39:96–115.
- Jasper H, Penfield W. Electro-corticograms in man: Effect of voluntary movement upon the electrical activity of the precentral gyrus. *Arch für Psych und Zeit Neurologie*. 1949; 183:163–174.
- Jensen O, Bonnefond M, VanRullen R. An oscillatory mechanism for prioritizing salient unattended stimuli. *Trends Cognitive Sci*. 2012; 16(4):200–206.
- Jensen O, Kaiser J, Lachaux J. Human gamma-frequency oscillations associated with attention and memory. *Trends Neurosci*. 2007; 30(7):317–324. [PubMed: 17499860]
- Jensen O, Mazaheri A. Shaping functional architecture by oscillatory alpha activity: gating by inhibition. *Front Hum Neurosci*. 2010; 4:1–8. [PubMed: 20204154]
- Jokisch D, Jensen O. Modulation of gamma and alpha activity during a working memory task engaging the dorsal or ventral stream. *J Neurosci*. 2007; 27(12):3244–3251. [PubMed: 17376984]
- Klimesch W, Doppelmayr M, Russegger H, Pachinger T. Theta band power in the human scalp EEG and the encoding of new information. *NeuroReport*. 1996; 7:1235–1240. [PubMed: 8817539]
- Kovach CK, Tsuchiya N, Kawasaki H, Oya H, Howard MA, Adolphs R. Manifestation of ocular-muscle EMG contamination in human intracranial recordings. *NeuroImage*. 2011; 54:213–233. [PubMed: 20696256]
- Lachaux JP, Axmacher N, Mormann F, Halgren E, Crone NE. High-frequency neural activity and human cognition: Past, present, and possible future of intracranial EEG research. *Prog Neurobiol*. 2012; 98:279–301. [PubMed: 22750156]
- Lancaster JL, Woldorff MG, Parsons LM, Liotti M, Freitas CS, Rainey L, Fox PT. Automated Talairach atlas labels for functional brain mapping. *Hum Brain Mapp*. Jul; 2000 10(3):120–131. [PubMed: 10912591]
- Legewie H, Simonova O, Creutzfeldt OD. EEG changes during performance of various tasks under open and closed eyes conditions. *Electroenceph Clin Neurophysiol*. 1969; 27:470–479. [PubMed: 4187033]
- Lopes Da Silva FH. Neural mechanisms underlying brain waves: from neural membranes to networks. *Electroenceph Clin Neurophysiol*. 1991; 79:81–93. [PubMed: 1713832]
- Lopes Da Silva FH, van Leeuwen WS. The cortical source of the alpha rhythm. *Neurosci Lett*. 1977; 6:237–241. [PubMed: 19605058]

- Lopes Da Silva FH, van Lierop TH, Schrijer CF, van Leeuwen WS. Organization of thalamic and cortical alpha rhythms: spectra and coherences. *Electroenceph Clin Neurophysiol.* 1973; 35:627–639. [PubMed: 4128158]
- Manning JR, Jacobs J, Fried I, Kahana MJ. Broadband shifts in LFP power spectra are correlated with single-neuron spiking in humans. *J Neurosci.* 2009; 29(43):13613–13620. [PubMed: 19864573]
- Mantini D, Perrucci MG, Del Gratta C, Romani GL, Corbetta M. Electrophysiological signatures of resting state networks in the human brain. *Proc Natl Acad Sci U S A.* 2007; 104(32):13170–13175. [PubMed: 17670949]
- Miller KJ, Leuthardt EC, Schalk G, Rao RPN, Anderson NR, Moran DW, Ojemann JG. Spectral changes in cortical surface potentials during motor movement. *J Neurosci.* 2007; 27:2424–2432. [PubMed: 17329441]
- Miller KJ, Sorensen LB, Ojemann JG, den Nijs M, Sporns O. Power-law scaling in the brain surface electric potential. *PLoS Comput Biol.* 2009; 12; 5
- Moruzzi G, Magoun H. Brain stem reticular formation and activation of the EEG. *Electroenceph Clin Neurophysiol.* 1949; 1:455–473. [PubMed: 18421835]
- Mundy-Castle AC. The electroencephalogram and mental activity. *Electroenceph Clin Neurophysiol.* 1957; 9:643–655. [PubMed: 13480237]
- Nunez, PL.; Srinivasan, R. *Electric fields of the brain.* Oxford University Press; New York: 2006.
- Pfurtscheller G, Aranibar A. Evaluation of event-related desynchronization (ERD) preceding and following voluntary self-paced movement. *Electroenceph Clin Neurophysiol.* 1979; 46(2):138–146. [PubMed: 86421]
- Pfurtscheller, G.; Lopes Da Silva, FH. EEG Event-related desynchronization (ERD) and event-related synchronization (ERS). In: Niedermeyer, E.; Lopes Da Silva, FH., editors. *Electroencephalography: Basic principles, clinical applications, and related fields.* Williams & Wilkins; 1999. p. 1003-1016.
- Pfurtscheller G, Neuper C. Simultaneous EEG 10 Hz desynchronization and 40 Hz synchronization during finger movements. *NeuroReport.* 1992; 3:1057–1060. [PubMed: 1493217]
- Poulet JFA, Fernandez LMJ, Crochet S, Petersen CCH. Thalamic control of cortical states. *Nat Neurosci.* 2012; 15(3):370–372. [PubMed: 22267163]
- Poulet JFA, Petersen CCH. Internal brain state regulates membrane potential synchrony in barrel cortex of behaving mice. *Nature.* 2008; 454(7206):881–885. [PubMed: 18633351]
- Ray S, Maunsell J. Different Origins of Gamma Rhythm and High-Gamma Activity in Macaque Visual Cortex. *PLoS Biology.* 2011; 9(4):e1000610. [PubMed: 21532743]
- Schafer RJ, Moore T. Attention governs action in the primate frontal eye field. *Neuron.* 2007; 56:554–551.
- Smith JR. The electroencephalogram during normal infancy and childhood: II. the nature of the growth of the alpha waves. *The Pedagogical Seminary and Journal of Genetic Psychology.* 1938; 53:455–469.
- Stanton GB, Deng S-Y, Goldberg ME, McMullen NT. Cytoarchitectural characteristic of the frontal eye fields in macaque monkeys. *J Comp Neurol.* 1989; 282:415–427. [PubMed: 2715390]
- VanRullen R, Reddy L, Koch C. Attention-driven discrete sampling of motion perception. *Proc Natl Acad Sci U S A.* 2005; 102(14):5291–5296. [PubMed: 15793010]
- Volavka J, Matoušek M, Roubicék J. Mental arithmetic and eye opening. an EEG frequency analysis and GSR study. *Electroenceph Clin Neurophysiol.* 1967; 22:174–176. [PubMed: 4163688]
- Yuval-Greenberg S, Tomer O, Keren AS, Nelken I, Deouell LY. Transient induced gamma-band response in EEG as a manifestation of miniature saccades. *Neuron.* 2008; 58(3):429–441. [PubMed: 18466752]

Highlights

- Eye closure is known to have dramatic effects on the EEG, particularly in the α (8-12 Hz) band; to elucidate its effect on the brain, we recorded electrocorticograms (ECoG) from epilepsy patients undergoing invasive monitoring while they sequentially closed and opened their eyes.
- In addition to finding the expected increase in α -range power over occipital cortex, we found that eye closure causes an anatomically widespread power increase for a broad range of low frequencies (2–30 Hz).
- At high frequencies eye closure causes an anatomically focal power decrease over occipital cortex and Brodmann areas 8 and 9.

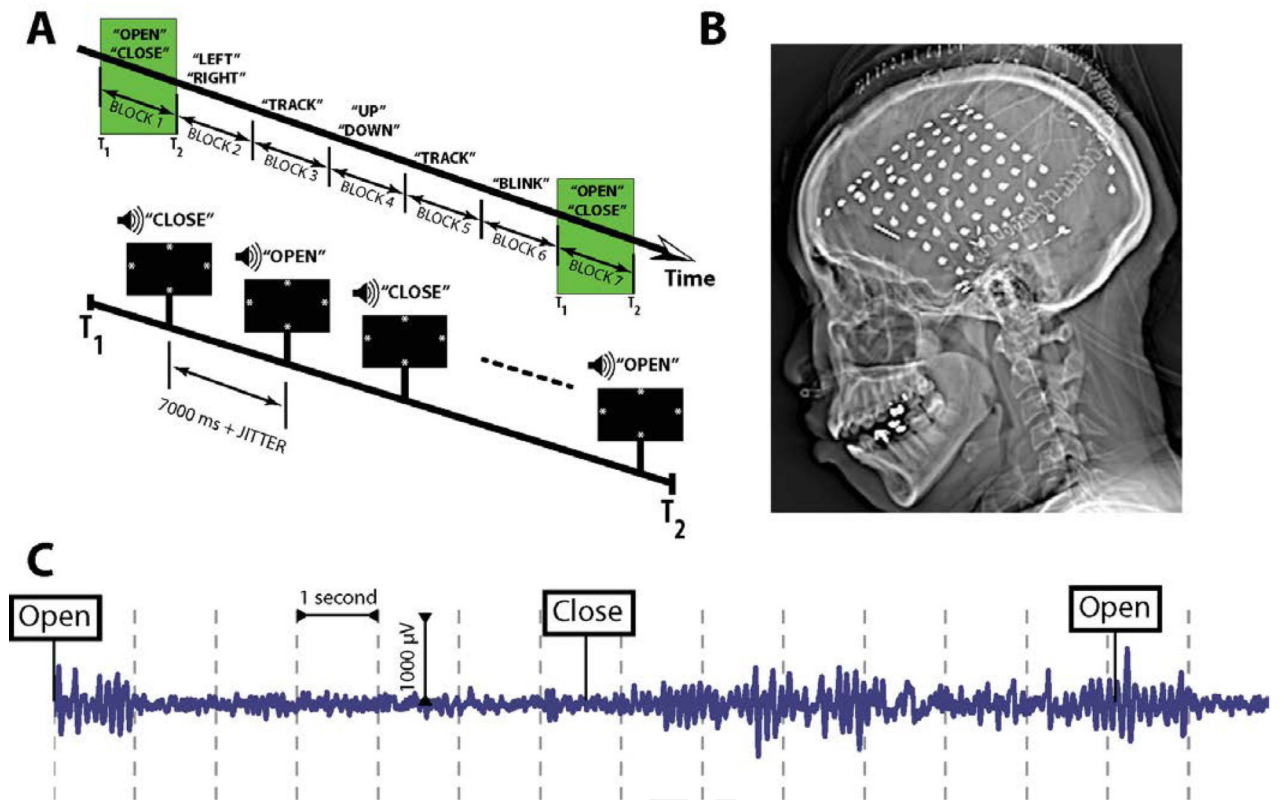


Figure 1. Behavioral task and data collection. **A:** Part of the oculomotor suite of tasks. Shown above, participants were played aural instructions to close/open their eyes and look to the left/right, and were also shown a meandering asterisk which they were to track with their eyes. Not shown are the cues to look left/right or up/down. **B:** Example radiographic image of a participant's electrode arrangement. **C:** Single electrode from Brodmann area 19 during performance of several eye closure trials.

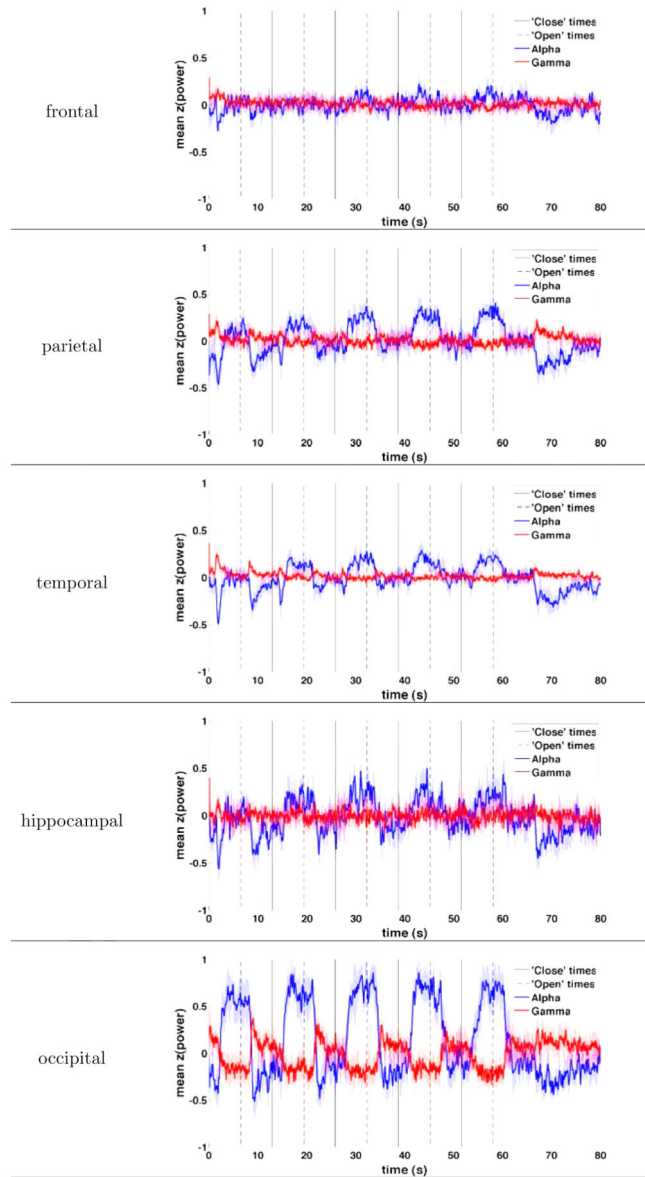


Figure 2.

Instantaneous power in the α and γ bands during the performance of the task, shown for electrodes in frontal, parietal, temporal, hippocampal and occipital cortex. α power rises approximately 2s after the instruction to close eyes, with maximal effect over occipital, parietal and temporal cortex. γ power falls with similar time constant, appreciable only over occipital cortex.

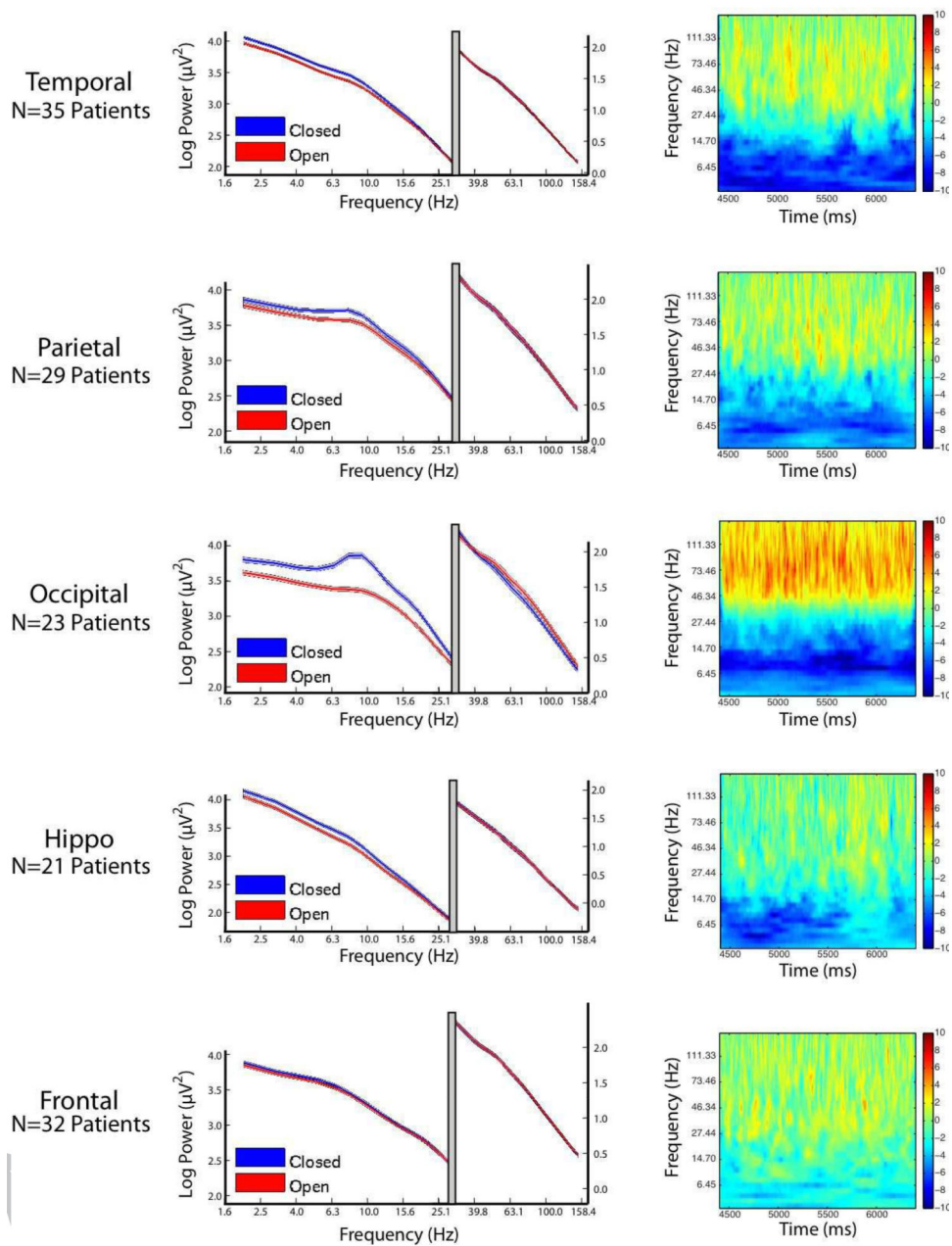


Figure 3. Power Spectral Density (PSD) and Time-Frequency Spectrograms for the epoch from 4400 to 6400 ms post-instruction. Each row represents a distinct anatomical area, as indicated on the left side of the figure. Left panel: PSDs demonstrating spectral power for each area is shown for all eyes open events (red) and all eyes closed events (blue), averaged across all participants. Shaded width of line represents 95% CI. To allow greater detail on the PSDs at high frequencies, the x-axis is split with a modified y-axis scale for high frequencies. Right panel: the time-frequency plots represent the difference in power between the eyes-open and eyes-closed condition, across time. Red colors represent more power during eyes-open, and blue colors represent more power during eyes-closed.

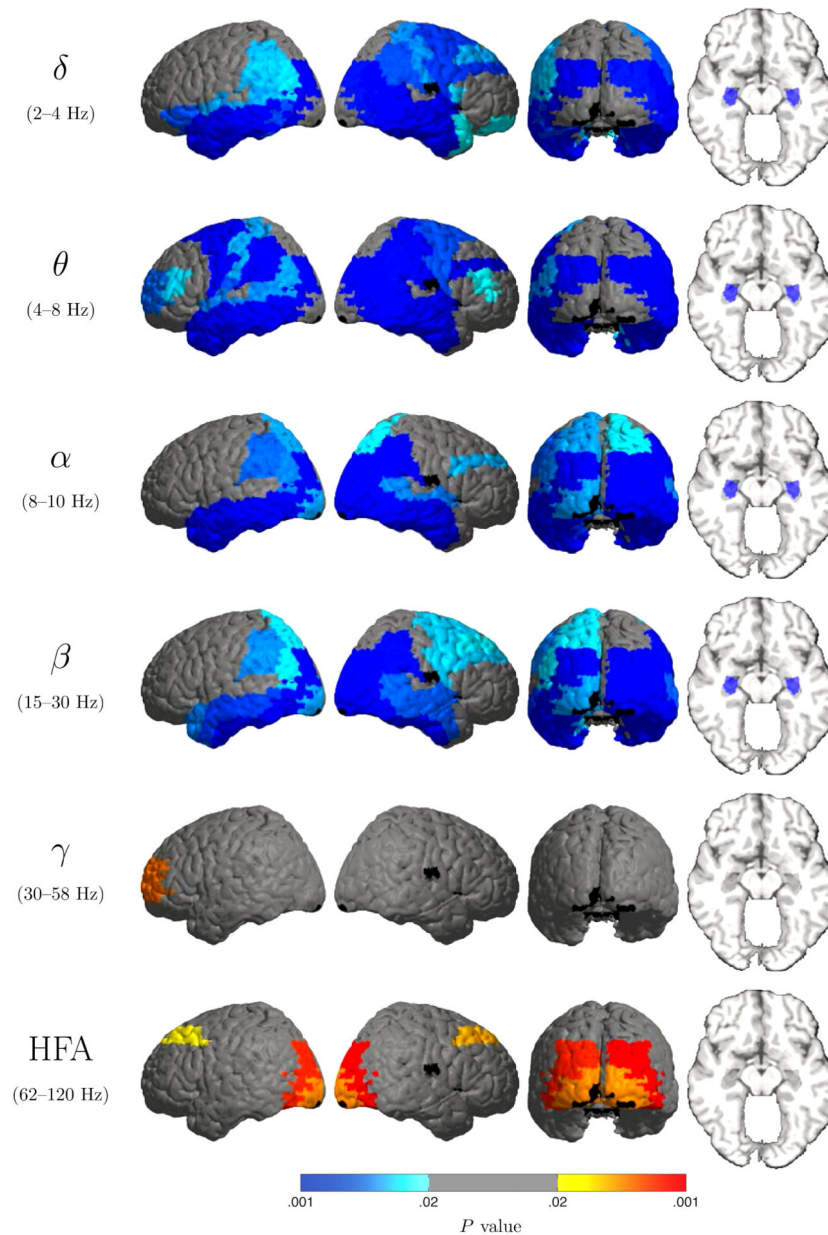


Figure 4.

P values for comparison of power during eyes closed vs. eyes open, shown for each Brodmann area (BA). The maps show diffuse power increase during eye closure (blue shades) over multiple low-frequency bands, extending postero-anteriorly from occipital cortex to the temporal poles bilaterally and including the hippocampi. (BA 17 is not significant under this analysis due to insufficient electrode coverage in this patient cohort.) A simultaneous power decrease (orange/red) at high frequencies, most prominently in the HFA band, over occipital cortex and Brodmann area 8. The sole significant region in the γ (30–58 Hz) band is left Brodmann area 9.

Table 1

Electrocorticographic patient database for the trackball task. For each participant, the identification number (**ID**), gender, age, handedness, number of bipolar electrode pairs (**# BPD**), pass-band of the amplifier's filter settings, and a brief anatomical description of the electrode coverage are listed. **TJUH**: Thomas Jefferson University Hospital; **HUP**: Hospital of the University of Pennsylvania;

| ID | Gender | Age | Handedness | # BPD | pass-band (Hz) | Electrode Coverage |
|-----------|---------------|------------|-------------------|------------------|-----------------------|---------------------------------------------------|
| TJUH 1 | F | 40 | R | 88 | 0.5 - 100 | b/l Depths; b/l Temp Strips |
| TJUH 2 | M | 39 | L | 43 | 0.5 - 100 | b/l Depths; L Fron + b/l Temp Strips |
| TJUH 3 | F | 34 | R | 95 [†] | 0.5 - 100 | b/l Depths; R Front-Temp-Par Strips |
| TJUH 4 | F | 39 | R | 114 | 0.5 - 100 | R Front-Temp-Par Strips; L Temp Strips |
| TJUH 5 | M | 29 | R | 35 | 0.5 - 100 | L Front-Temp Strips |
| TJUH 6 | F | 25 | R | 143 | 0.5 - 100 | L Front-Temp-Par Grid + Front-Temp Strips |
| TJUH 7 | M | 43 | R | 68 | 0.5 - 100 | b/l Depths; R Temp-Occip Strips |
| TJUH 8 | M | 21 | R | 129 | 0.5 - 100 | b/l Front-Temp Grid + Strips |
| TJUH 9 | M | 56 | R | 43 | 0.5 - 100 | L Depths; L Temp-Occip Strips |
| TJUH 10 | M | 20 | R | 139 [†] | 0.03 - 300 | b/l Depths; b/l Temp-Front Strips |
| TJUH 11 | M | 41 | R | 84 | 0.03 - 600 | R Depths; R Temp-Par-Occip Strips |
| TJUH 12 | F | 34 | R | 95 | 0.03 - 600 | L Depths + Temp Grid + Strips |
| TJUH 13 | F | 52 | R | 95 | 0.03 - 600 | R Depths + Front-Temp Grid |
| TJUH 14 | M | 44 | R | 92 | 0.03 - 600 | R Depths; b/l Temp-Front Strips |
| TJUH 15 | M | 35 | R | 121 | 0.03 - 600 | b/l Front-Par Strips |
| TJUH 16 | F | 44 | R | 53 | 0.03 - 600 | b/l Depths; b/l Temp Strips |
| TJUH 17 | M | 33 | R | 105 | 0.03 - 600 | b/l Front-Temp-Par Strips |
| TJUH 18 | F | 23 | R | 94 | 0.03 - 600 | R Depths + Grid; b/l Temp Strips |
| TJUH 19 | F | 48 | R | 84 | 0.03 - 600 | b/l Temp-Front-Occip Strips |
| TJUH 20 | M | 33 | R | 46 | 0.03 - 1200 | L Temp Strips + STG Depths |
| TJUH 21 | M | 45 | R | 86 | 0.03 - 600 | b/l Depths; b/l Temp-Front Strips |
| TJUH 22 | M | 53 | R | 83 | 0.03 - 600 | b/l Depths; b/l Temp Strips |
| TJUH 23 | M | 29 | R | 63 | 0.03 - 600 | L Front + b/l Temp Strips |
| TJUH 24 | M | 35 | R | 90 | 0.03 - 600 | b/l Depths; b/l Fron-Temp Strips |
| TJUH 25 | F | 48 | R | 133 [†] | 0.03 - 600 | b/l Depths; b/l Fron-Temp-Par + R Occip Strips |
| TJUH 26 | F | 20 | R | 126 | 0.03 - 600 | R Depths; b/l Fron-Temp Strips |
| TJUH 27 | M | 35 | L | 117 [†] | 0.03 - 600 | L Temp Grid + Fron-Temp Strips |
| HUP 1 | F | 27 | R | 40 | 0.16 - 134 | b/l Depths; b/l Front-Temp Strips |
| HUP 2 | M | 27 | R | 68 | 1.6 - 134 | b/l Depths; b/l Front-Temp Strips |
| HUP 3 | M | 20 | L | 130 | 1.6 - 134 | L Fron Grid + |

| ID | Gender | Age | Handedness | # BPD | pass-band (Hz) | Electrode Coverage |
|-------|--------|-----|------------|-------|----------------|---------------------------------|
| | | | | | | Fron-Temp Strips + R fron Strip |
| HUP 4 | M | 37 | R | 123 | 1.6 - 134 | R Temp-Front-Par Grid + Strips |
| HUP 5 | F | 30 | L | 58 | 1.6 - 134 | b/l Fron-Temp-Occip Strips |

[†]The electrode montage was changed during the hospital stay. The second montage from patient TJUH 3 contained 81 bipolar derivations. The second and third montage from patient TJUH 10 contained 50 and 139 bipolar derivations, respectively. The second montage from patient TJUH 25 contained 133 bipolar derivations.